

Large scale natural gas emplacement traced by noble gases: the Virunga Volcanic Province

Research Thesis

Presented in partial fulfillment of the requirements for graduation

“with Research Distinction in Geological Science” in the undergraduate colleges of
The Ohio State University

By

Erica Lynn Maletic

The Ohio State University

May 2015

Project Advisor: Dr. Thomas Darrah, School of Earth Sciences

Abstract

Enhanced oil recovery (EOR), sometimes called tertiary recovery, involves the injection of miscible fluids such as carbon dioxide (CO₂) into previously produced hydrocarbon reservoirs. EOR commonly prolongs the life of petroleum reservoirs globally, in some instances nearly doubling the amount of petroleum initially recovered with conventional methods and water flooding. As a result, today, carbon dioxide reservoirs with sufficient volume and pressure to provide EOR fluids are a resource that is in an increasingly high demand.

For these reasons, the development of geochemical techniques, capable of better characterizing the source and the history of CO₂ reservoir filling, trapping, and producible volumes is critical to the future economic success of EOR and the petroleum industry in general. In order to explore successfully for economically viable CO₂ fields, one needs to understand the sources, emplacement history, and subsequent tectonic evolution of a CO₂ reservoir. These factors can be determined by understanding the magmatic source of CO₂ gases, the isotopic composition of the CO₂ gas, the stratigraphic and structural conditions of reservoir trapping, and the volume of CO₂ that is present in reservoirs today.

The Virunga Volcanic Province (VVP), located along the western branch of the East African Rift System (EARS), provides an example of a currently filling CO₂ reservoir. As a result, it represents an appropriate place to study the source, migration, and emplacement of CO₂ reservoirs and validate many currently applied geochemical techniques. Throughout the last forty years, the Virunga Volcanic Province has experienced intense volcanic activity, which has led to significant interest in volcanic hazard activity in this region. For this project, we examined the major and trace element geochemistry of volcanic products and fumarole gases to evaluate the source and emplacement of CO₂ into the Earth's crust in the VVP. This study provides a comprehensive dataset of gas geochemistry for potential magmatic and geothermal sources, isotopic tracers of subsurface CO₂ migration, reservoir

infilling, and water-gas interactions. Specifically, my data include major gas compositions (CO_2 , N_2 , O_2 , H_2), noble gases (abundance and isotopic composition such as (e.g., $^3\text{He}/^4\text{He}$, $\text{CO}_2/^3\text{He}$, $\text{CH}_4/^3\text{He}$, $^{40}\text{Ar}/^{36}\text{Ar}$, $^{40}\text{Ar}^*/^4\text{He}$)), and stable isotope geochemistry ($\delta^{13}\text{C}\text{-CO}_2$) from fumaroles on Mount Nyiragongo and throughout the region to evaluate the sources that feed magmatic systems across the VVP and major and trace element data for a time series of lava samples taken from Nyamuragira (2006 and 2010 eruptions) and Nyiragongo (2002 eruptions and lava lake samples from 2005 and 2010).

Acknowledgements

I would first like to thank my research advisor, Dr. Tom Darrah, for giving me the opportunity to work on this project in a unique geological setting. He introduced me to an entirely different part of geology that I was not aware of and that turned out to be one of the most interesting things I have learned during my college career. He also had the ability to help me absorb information quickly and was able to push me to achieve more than I thought I could.

I would also like to recognize Dr. John Olesik, Dr. Jeremy Williams, Mr. Anthony Lutton, and Mr. Yohei Matsui for their assistance in training me on the inductively coupled plasma optical emission spectrometer, inductively coupled plasma mass spectrometer, and the noble gas mass spectrometer. Their patience while teaching me how to prepare samples and how to operate these complicated instruments was greatly appreciated. Without them my research would not have been possible.

On a similar note, I would like to acknowledge the Ohio State University's School of Earth Sciences. This large institution never made me feel like I was just another face in the crowd because of the camaraderie between the students in the school and the faculty. I know I have made many friendships that will last a lifetime thanks to the open and welcoming atmosphere that was always encouraged during my time here.

A large thank you goes to the Shell Exploration and Production Company for the opportunity to work for eight weeks, in 2014, with the Shell Undergraduate Research Experience. The internship allowed me to get a huge amount of work done and I would not have completed this research without the opportunity. Similarly, I would like to thank Dr. Dario Tedesco and Dr. Robert Poreda for providing me access to their samples and to the United Nations Office for Project Services (UNOPS) for providing the travel support for my sample collection in the field.

Lastly, I would like to give special thanks my family and friends. My parents continually encouraged me to strive for greatness and have made me the person I am today. As for my friends, I

would not have made it through the stress of the main geology sequence (mineralogy, petrology, structure, and field camp) without your support. I'll never forget the late night coffee runs and the sleep deprived shenanigans while studying for a big test or trying to get a lab in on time. It's been a fun ride.

Table of Contents

Abstract.....	i
Acknowledgements.....	iii
List of Figures.....	vi
Introduction.....	1
Enhanced Oil Recovery (Tertiary Recovery).....	4
Geological Setting of the Virunga Volcanic Province.....	5
Methods.....	7
Sample Collection.....	7
Analysis and Techniques.....	7
Results.....	11
Major Element Composition of the Volcanic Source Rocks.....	11
Trace Element Composition of the Volcanic Source Rocks.....	11
Source Comparison with Gases.....	13
Migration of Gases.....	13
Discussion.....	15
Source Rock Composition.....	15
Variability in Metasomatic Influence over Time.....	16
Gas Migration.....	16
Conclusions.....	18
References.....	19

List of Figures

1. Map of study area.....	22
2. Total Alkali Versus Silica Diagram.....	23
3. REE plot.....	24
4. Th/U vs. Zr/Hf.....	25
5. Chemical Composition Throughout Time.....	26
6a. $^3\text{He}/^4\text{He}$ vs. Zr/Hf.....	27
6b. $^3\text{He}/^4\text{He}$ vs. Th/U.....	27
8. $\text{CO}_2/^3\text{He}$ vs. $\delta^{13}\text{C}-\text{CO}_2$	28

Introduction

Carbon dioxide (CO₂) is a major component of carbon in the Earth's mantle and crust and the second most abundant volatile in the mantle (only behind water). The distribution and cycle of CO₂ in the atmosphere and crust are controlled by many critical processes, which are as diverse as global warming, continental weathering, and plate subduction. As a result, understanding the distribution and interactions of CO₂ in the crust is critical to the successful management of anthropogenic CO₂ (Sherwood-Lollar and Ballentine, 2009).

Though seemingly an easy task, understanding the sources and basin scale processes that regulate the distribution of CO₂ in the crust is quite challenging because of CO₂'s multiple origins. These sources can include methanotrophy, oil field biodegradation, kerogen decarboxylation, hydrocarbon oxidation, decarbonation of marine carbonates and the degassing of magmatic bodies (Jenden et al., 1993; Gilfillan, 2009). Many of these sources can be distinguished by the $\delta^{13}\text{C}$ values, but natural gas fields that contain large concentrations of CO₂ generally lie in the overlapping range between carbonate breakdown and magmatic degassing, and the sources cannot easily be distinguished (Gilfillan et al, 2008).

Additionally, because of the highly soluble and reactive nature of CO₂, the extent of the interaction with the groundwater and other crustal minerals is not well constrained, yet these properties represent a significant parameter in evaluating CO₂ sinks. The groundwater systems associated with these CO₂ natural gas deposits are often comparable to oil and gas field brines and there are few techniques available to calculate regional groundwater movement through age, residence time, or the groundwater volumes that have interacted with the gas trapped in the reservoir (Gilfillan et al, 2009). By combining $\delta^{13}\text{C}$ -CO₂ with noble gas analyses one can provide further insights on the source of carbon dioxide (Gilfillan et al., 2008; Zhou et al., 2012; Gilfillan et al., 2009).

Noble gases (because of their low concentrations and chemical inertness) can serve as reliable tracers of these sources when paired with an in depth understanding of the processes that control their concentrations and isotopic compositions in different environments. Their origins have been well characterized to three specific sources: atmospheric (air-saturated water), crustal (radiogenic), and primordial (mantle-derived).

Atmospheric noble gases (e.g., ^{20}Ne , ^{36}Ar) can enter the subsurface via dissolution into ground or pore waters, termed air-saturated water. The air-saturated water (ASW) composition of groundwater is constant globally for both concentration and isotopic composition. As a result, the concentrations of ASW components in crustal water are a well-constrained function of temperature, salinity, and atmospheric pressure (elevation). Atmospheric noble gases (AIR) dissolve in groundwater when meteoric water equilibrates with the atmosphere prior to recharge into the subsurface. This equilibration follows Henry's Law, with solubility increasing with higher atomic mass: $\text{He} < \text{Ne} < \text{Ar} < \text{Kr} < \text{Xe}$ (Craig and Weiss, 1971).

Shallow groundwaters typically have ASW noble gas composition characterized by near solubility levels of $[\text{He}]$ ($\sim 40\text{-}45 \times 10^{-6} \text{ cm}^3 \text{ STP/L}$), $[\text{Ne}]$ ($175\text{-}220 \times 10^{-6} \text{ cm}^3 \text{ STP/L}$), and $[\text{Ar}]$ ($0.28\text{-}0.49 \text{ cm}^3 \text{ STP/L}$). Isotopically each gas component is similar to atmospheric compositions (i.e., helium: $^3\text{He}/^4\text{He} = 1.36 \times 10^{-6}$ or $\sim 0.985Ra$ (where Ra is the ratio of a sample relative to AIR = 1.39×10^{-6}); neon: $^{20}\text{Ne}/^{22}\text{Ne}$ (~ 9.8) and $^{21}\text{Ne}/^{22}\text{Ne}$ (~ 0.0289); and argon: $^{38}\text{Ar}/^{36}\text{Ar}$ (~ 0.188) and $^{40}\text{Ar}/^{36}\text{Ar}$ (~ 295.5)). With the exception of helium ($0.985Ra$), the isotopic effect related to Henry's Law solubility dissolution into meteoric water is less than the measurement error for Ne and Ar.

Crustal or radiogenic isotopes (e.g., ^4He , $^{21}\text{Ne}^*$ and $^{40}\text{Ar}^*$) are produced by the decay of radioactive elements. As CO_2 or meteoritic fluids interact with crustal fluids, the noble gas composition changes through the radiogenic nature and geologic history of the rocks through which fluids migrate within the Earth's crust (i.e., termed crustal gases). Crustal gases are produced from the

decay of $^{235, 238}\text{U}$, ^{232}Th ($^4\text{He}^*$ (α -decay) and $^{21}\text{Ne}^*$ (α -n reactions)) and K ($^{40}\text{Ar}^*$ (electron capture)) at known decay rates. The Earth's crust is typically enriched in uranium content (specifically in comparison to thorium) as a result of uranium adsorption onto organic-rich particles during sediment deposition. In the crust, the typical range of concentrations are: uranium ($\sim 1\text{-}30$ ppm), thorium ($\sim 1\text{-}30$ ppm), and ^{40}K (total K $\sim 26,000$ ppm, with a $[^{40}\text{K}] / \text{K}$ ratio of $1.170 \times 10^{-4} = \sim 3$ ppm of ^{40}K of which 11% decays to $^{40}\text{Ar}^*$) (Taylor and McLennan 1995). Radioactive decay leads to characteristic ratios of these radiogenic gases in crustal rocks (Hunt et al., 2012). Typical isotopic ratios of crustal noble gases are $^3\text{He}/^4\text{He} = \sim 0.01\text{Ra}$, $^{20}\text{Ne}/^{22}\text{Ne}$ ($\sim 9.7\text{-}10.0$), $^{21}\text{Ne}/^{22}\text{Ne}$ ($\sim 0.029\text{-}0.060$), and $^{40}\text{Ar}/^{36}\text{Ar}$ ($\sim 295.5\text{-}1100$), respectively (Darrah et al., 2013; Ballentine et al., 1991).

Mantle or primordial gases (e.g., ^3He) were derived from meteoritic and cosmogenic sources prior to the accretion of the Earth and have been steadily degassing with mantle-derived rocks and fluids ever since (Lupton and Craig, 1975; Ballentine et al., 2002). The most common example of a primordial gas is ^3He (Ballentine et al, 2002).

The unique signature, determined by elemental and isotopic compositions of the three noble gas sources, allows for their contributions to be quantified in a CO_2 fluid (or other crustal fluid) and provides information on potential sources that could otherwise be indeterminable (Ballentine and Burnard, 2002). Once incorporated into crustal fluids, isotopic fractionation of noble gases from any of these sources occurs during some aspect of fluid migration (e.g., advection, diffusion). As a result, noble gases can also be used to constrain residence times of natural gas associated water and to calculate the degree of interaction between a crustal fluid and the ground water system (Gilfillan et al, 2009).

Today, at the same time many scientists are concerned about increasing atmospheric release of the CO_2 , a potent greenhouse gas, the industrial use of the gas is rapidly increasing largely in response to enhanced oil recovery (EOR), which is the injection of miscible fluids such as CO_2 into

previously produced hydrocarbon reservoirs in the Earth's crust. The injection of CO₂ significantly prolongs the life of petroleum reservoirs and increases the amount of recoverable oil and gas (Bondor, 1992).

As a result of increased utilization of CO₂, it is critical to identify, characterize, and exploit new geological CO₂ reservoirs. The development of geochemical techniques capable of better characterizing the source and history of CO₂ reservoir filling and trapping is critical to the future economic success of EOR and the petroleum industry in general. One needs to understand the sources (specifically magmatic sources), emplacement history, and subsequent tectonic evolution of a CO₂ reservoir in order to conduct CO₂ exploration. These factors can be determined by understanding the isotopic composition of the gas, the stratigraphic and structural conditions of reservoir trapping, and the volume of CO₂ that is present in the reservoir today (Gilfillan et al, 2009).

Enhanced Oil Recovery (Tertiary Recovery)

Most conventional hydrocarbon reservoirs have already undergone primary hydrocarbon recovery, which usually relies on overpressure of the formation or mechanical pumping (Bondor, 1992). Primary hydrocarbon recovery typically produces only about 10 percent of a reservoir's oil-in-place. Secondary hydrocarbon recovery can recover 20 to 40 percent of the oil-in-place by injecting water into the reservoir to displace the oil, commonly called water flooding. The goal of EOR (or tertiary recovery) is to improve the production of hydrocarbons emplaced within the formation. The most frequently used and economical methods of EOR commonly involves the injection of miscible fluids such as CO₂. This method increases the reservoir pressure, the CO₂ mixes with the remaining hydrocarbons to decrease the viscosity, and ultimately increases the flow rate out of the reservoir. Gas injection EOR accounts for almost 60 percent of EOR production in the United States and can

recover 30 and 60 percent or more of the oil in the reservoir (Bondor, 1992), commonly more than is produced by either primary or secondary recovery.

Many large CO₂ reservoirs are already being heavily exploited. One of the largest reservoirs in the world, McElmo Dome (Four Corners, USA), has approximately 476 billion m³ (17 trillion cubic feet (TCF)) of total reserves, 98 percent of which is CO₂, and has a production of 1.1 billion cubic feet per day (BCFD) (USDOE, “Subsurface Sources”). Another unusually large reservoir is Jackson Dome (MS, USA) with a total of 6.1 TCF (also containing 98 percent CO₂) and is being produced at a rate of 0.9 BCFD as of 2012 (USDOE, “Near-Term Projection”).

Though these reservoirs are enormous in size, there will come a time, likely in the next 20 years, when the gas has all been recovered, as the rate of recovery far exceeds even the most optimistic the rates of gas migration into the reservoir. In order to continue to meet industrial demands for EOR, new CO₂ reserves must be identified and exploited. With the increase in demand for this resource over the last decade, development of geological, geophysical, and geochemical techniques capable of determining the source, emplacement (migrational history), and retention of CO₂ reserves is critical to the economic success of CO₂. One example of a geologically active and actively charging CO₂ field is the volcanically and kinematically active Virunga Volcanic Province located along the western branch of the East African Rift System.

Geological Setting of the Virunga Volcanic Province

The western branch (WB) of the East African Rift System (EARS) is a seismically active 3,000 km long segment that is proximal to the suture zone between the Archaean Tanzania craton and the Proterozoic Nubian plate (Tedesco et al., 2010) (Figure 1). The WB can be divided into four main volcanic districts: the Toro-Ankole region (western Uganda), the Virunga (at the border of the Democratic Republic of the Congo (DRC) and Rwanda), the Kivu provinces (at the border between

DRC, Uganda, Rwanda, and Burundi), and the Rungwe field (Tanzania). These regions consist of unusual silica-undersaturated lavas with ultrapotassic, hypersodic, and carbonatitic components (Furman, 2007, Chakrabarti et al, 2009).

Due to the increase in volcanic activity in the VVP throughout the last forty years and to its proximity to the city of Goma (now with more than 2 million inhabitants), extensive attention has been directed towards the VVP. Data collected as part of the United Nations (UNOPS)-funded mission throughout the last dozen years have provided an unrivaled opportunity for sampling and unprecedented access to samples and the data from the region. These samples include fumarolic gas, water, and rocks samples from volcanic and geothermal sources throughout the region, which provide an opportunity to examine the source of CO₂, its migration in the subsurface, and the spatial relationship between volatiles and their structural traps.

Here, we present major (e.g., K, Na, Si), trace element (REEs, HFSE's, U, Th), and gas geochemical data (e.g., ³He/⁴He, CO₂/³He, CH₄/³He, ⁴⁰Ar/³⁶Ar, ⁴⁰Ar*/⁴He) from volcanic products and fumaroles within the region. Most of the data are presented in a time series from 2002 to 2010, including eruptions at Mt. Nyamuragira (2006 and 2010) and Mt. Nyiragongo (2002 in addition to 2005, 2006, and 2010 lava lake sample collections).

These data from these samples allowed us to characterize the mantle sources that feed magmatic systems and produce the rare lava compositions across the VVP. These data also allow us to evaluate how the geochemistry changes throughout this volcanically active time period.

Methods

Sample collection

Volcanic rock samples were collected from freshly erupted products at Mt. Nyamuragira in 2006 and 2010 and from Mt. Nyiragongo in 2002 after samples had solidified. Lava lake samples were collected from Mount Nyiragongo by descending a 1 meter long titanium rod into the active lava lake either via a rope pulley system or by hand in 2006 and 2010.

Gas samples were collected using an inverted high density polyethylene (HDPE) funnel connected to pre-evacuated 100 mL borosilicate flasks (connected by silicone/Tygon[®] tubes) with a teflon stopcock and was filled with a 40 mL of 4 M NaOH and 0.15 M Cd(OH)₂ aqueous suspension (Giggenbach and Goguel, 1989, and Montegrossi et al., 2001). Gas data are reported on a water-free basis due to the water vapor being fixed by relatively low discharge temperature and is therefore not considered part of the gas composition. Two samples were collected at each sampling point and analyzed in the University of Florence and the Istituto Nazionale Vulcanologia Geofisica of Naples, Italy (for chemical composition, carbon isotopic composition of CO₂, and nitrogen isotopic composition of N₂) and in the Water Health Energy and Environment Laboratory at The Ohio State University (USA) (isotopic ratios of noble gases (He, Ne, Ar, Kr, Xe)) following standard methods (Darrah et al., 2013).

Analysis and techniques

All the whole rock samples of this study were powdered in an alumina Spex[™] ball mill. The samples were measured using an inductively-coupled plasma (ICP) optical emission spectrometry. Trace element concentrations were measured using a quadrupole ICP mass spectrometer (Thermo elemental X-7 series) at the University of Rochester. 25-mg of rock powder for each sample was

digested in 2:1 HF/HNO₃ acid mixtures and sealed in teflon beakers on a hotplate for 48 hours. After evaporation to initial dryness, the samples were treated twice with 1 ml of HNO₃ and dried down. Each sample was diluted to 100 ml of 2% HNO₃ solution (dilution factor 4000) with ~ 10 ppb internal standard of In, Cs, Re, and Bi. The concentrations of the various elements, other than the rare earth elements, are within 5% error, as estimated from repeated measurements of AGV-2 (andesite-USGS) and BHVO-2 (basalt-USGS) rock standards which were run as unknowns. The rare earth elements (REEs) are more precisely determined to within 2% error. Oxide correction was necessary for the REEs, and the sizes of the oxide and hydroxide interferences were estimated by analyzing single element solutions of the REEs. Lower limits of detection for the elements reported are typically less than 5 ppb (Chakrabarti et al., 2009).

A Shimadzu 14A gas chromatograph (GC) with a 10 m long stainless steel column (2 mm) packed with a Chromosorb PAW 80/100 mesh coating with a 23% SP 1700 and a flame ionization detector (FID) was used to analyze hydrocarbons (including CH₄, C₂H₆, to C₆H₁₄). Concentrations of N₂, O₂, H₂, and Ar were determined using a Shimadzu 15A GC with a 10 m long 5A molecular sieve column and a thermal conductivity detector (TCD). The solution was separated from the precipitate by means of centrifugation to determine CO₂ as CO₃²⁻ by titration (Metrohm Basic Titrino) with 0.5 M HCl solution, in addition to H₂S by first oxidizing CdS to SO₄²⁻ with H₂O₂ and then using ion chromatography (Tedesco, 1994, Montegrossi et al., 2001, Tassi et al., 2010, and Tassi et al., 2011). All data reported have an analytical uncertainty of less than 5%.

By adding approximately 5 mL anhydrous phosphoric acid to 2 mL of the soda solution under vacuum, this technique allowed the emitted CO₂ to equilibrate at 25 ± 0.1 °C in a thermal bath overnight and then the carbon isotopic composition (¹³C/¹²C) of CO₂ (expressed as δ¹³C–CO₂ ‰ (per mil) V-PDB) was determined. The extracted CO₂ was purified using liquid N₂ and N₂-trichloroethylene cryogenic traps and analyzed using a Finnigan Delta S mass spectrometer (MS).

Internal (Carrara and San Vincenzo marbles) and international (NBS10 limestone, and MBS19 carbonate) standards were used to estimate the external precision. The reproducibility and analytical precision were $\pm 0.1\text{‰}$ and 0.05‰ , respectively (Capaccioni et al., 2011 and Aguilera et al., 2012).

Elemental and isotopic compositions of the noble gases were analyzed on a Thermo Fisher Helix SFT Noble Gas MS, fitted with an electron multiplier and pulse counting electronics on the axial collector by previously described methods (Darrah and Poreda, 2012) at The Ohio State University. A $77\text{ }\mu\text{cm}^3$ air standard at STP was used prior to the gas analysis to tune mass calibrations, minimize the formation of doubly charged species (e.g. $^{40}\text{Ar}^{2+}$ and CO_2^{2+}), and quantify isobaric interferences on neon (Ne) isotopes at less than 5%. The Ne isotopic composition was corrected by measuring $[^{40}\text{Ar}^+]$ and $[\text{CO}_2^+]$ and subtracting the quantified production ratio for each of the doubly charged species by methods reported previously (Darrah and Poreda, 2012). Other potential interferences were similarly monitored and corrected (e.g., HF and H₂O).

Gas samples were purified in a high vacuum line for the analysis of noble gases constructed with 316 stainless steel, used to minimize He diffusion. Water vapor and CO₂ were trapped cryogenically at $-90\text{ }^\circ\text{C}$ and $-195\text{ }^\circ\text{C}$, respectively, while bulk gases, like N₂ and O₂, were purified by sequential exposure to a bulk Zr-Al getter (SAES ST-707) held at 450°C and a SAES SORB-AC cartridge also held at 350°C then cooled to 25°C using an activated charcoal finger. Once clear of reactive gases, Ne, Ar, and Kr were trapped on a stainless steel sintered, charcoal finger element at liquid nitrogen temperatures. The helium and neon were then expanded into the mass spectrometer and analyzed sequentially. After He and Ne analysis, Ar, Kr, and Xe were analyzed on a separate aliquot of samples.

The helium ($^3\text{He}/^4\text{He}$) isotope ratios (hereafter expressed as R/R_a ratios, where R is the $^3\text{He}/^4\text{He}$ measured ratio of the sample and R_a is the $^3\text{He}/^4\text{He}$ ratio of the air: 1.39×10^{-6}) (Clarke et al., 1969) were normalized to a Yellowstone Park standard (MM) provided by H. Craig (SIO) which

has been measured against air and a ratio of 16.5 ± 0.1 times the atmospheric ratio was obtained (as measured in five noble gas laboratories) using a Yellowstone Park standard ($R_{MM}/R_A = [^3\text{He} / ^4\text{He}_{MM}] / [^3\text{He} / ^4\text{He}_{air}]$) (Poreda and Farley, 1992).

Results

Major Element Composition of the Volcanic Source Rocks

Major element concentrations of volcanic were measured in 18 samples from around Mt. Nyiragongo and Mt. Nyamuragira. (Figure 2). A total alkali silica plot compares $\text{Na}_2\text{O} + \text{K}_2\text{O}$ vs. SiO_2 to determine the source of mantle-derived melts. Typically terrestrial volcanic samples fall along a trend of positive correlation between $\text{Na}_2\text{O} + \text{K}_2\text{O}$ vs. SiO_2 .

Most Mt. Nyamuragira samples have fallen consistently in the field of basanites to trachy-basalts (42-47 wt% SiO_2 , 5.5-7 wt% $\text{Na}_2\text{O} + \text{K}_2\text{O}$). By comparison, samples from Mount Nyiragongo, located <20 km away, have consistently displayed a slightly lower (<40 wt%) SiO_2 and slightly higher alkali content (6.5 - 7.8 wt%) (Figure 2).

The pre-1977 eruption samples range from approximately 38-41 wt% SiO_2 , and vary greatly in alkalinity, from 3-10 combined wt% $\text{Na}_2\text{O} + \text{K}_2\text{O}$. These samples have greater variability than the 2002 lava samples, containing 0.5 – 12 combined wt% $\text{Na}_2\text{O} + \text{K}_2\text{O}$ and 37-39 wt% SiO_2 . Up through the 2002 eruption, Mt. Nyiragongo rocks plot in the foidite field (outside the field of volcanic rocks that are commonly found) and trend toward rare, super-alkaline, carbonatite lavas in the total alkali versus silica diagram (LeMaitre, 1984). However, following the 2002 eruption, between 2006 and 2010, Mt. Nyiragongo lavas have continued to trend toward carbonatitic extremes for silica-undersaturated, alkali-rich rocks globally. In fact, only the purely carbonatitic Oldoino Lengia has a lower silica content amongst active volcanoes (Fischer et al., 2009).

Trace Element Composition of the Volcanic Source Rocks

Chondrite-normalized rare earth element (REE) patterns are commonly used to evaluate the source of volcanic products and to calculate the degree of partial melting. Rocks from both the

Nyiragongo and Nyamuragira volcanoes show light rare earth element (LREE) enrichment when normalized to chondrite (i.e., bulk earth) (Figure 3). Although the Nyamuragira samples are less enriched in LREE than the Nyiragongo ones, the REE concentrations are all abnormally high, with some LREE concentrations exceeding 100 ppm (approximately 1000x chondrite).

Elevated LREE patterns can suggest metasomatism of crustal materials, perhaps even sub-continental lithospheric inputs, either by melting of the crust or the recycling of subducted crustal materials. Some specific REE patterns, such as a gadolinium (Gd) anomaly, often provide clues that can distinguish metasomatism of crustally-derived volcanic products from extremely small partial melts. Because Gd preferentially complexes with supercritical CO₂, a Gd anomaly is often a signature of extensive mantle metasomatism. The REE plot shows a clear excess of Gd (i.e., a Gd anomaly), which most likely reflects either sub-continental lithospheric mantle or recycled Proterozoic crust (Figure 3).

In addition to REEs, other trace element ratios often provide into the source and degree of metasomatism. Several examples include Th/U, Nb/U, and Zr/Hf. When metasomatism occurs the Th/U and Nb/U decrease (an increase in [U]), while Zr/Hf increase (Zr increases). Thus by plotting Th/U vs. Zr/Hf, one can delineate trace element fractionation related to metasomatism. When Th/U vs. Zr/Hf are plotted against each other (Figure 4), there is a negative correlation between the Th/U and Zr/Hf ratios.

In addition to showing a relatively high degree of metasomatism, the plot of Th/U vs. Zr/Hf also shows a change in the degree of mantle metasomatism since Nyiragongo's last eruption in 2002 (Figure 4). The lavas show a progression over time in alteration by metasomatism and perhaps change in lava source material.

Source Comparison with Gases

Based on observations for changing major and trace element chemistry, we evaluated a time series of noble gas data, specifically helium isotopes from volcanic samples and gas fumaroles. Consistent with major and trace element data, the helium isotope values show a coherent pattern of change through time. Specifically, the $^3\text{He}/^4\text{He}$ values appear to change concomitantly with the trace element tracers of metasomatism (e.g., Zr/Hf, Nb/U, Th/U).

During periods of high metasomatism, the $^3\text{He}/^4\text{He}$ has a MORB-like composition ($\sim 8Ra$), while the $^3\text{He}/^4\text{He}$ have dropped to $\sim 6.5Ra$ (consistent sub-continental lithospheric mantle (SCLM)) as metasomatism values have decreased. As the tracers in the rocks decrease in metasomatic influence, the He isotope ratios in the gases decrease in Ra , returning to a more SCLM-like pattern (Figure 5, 6a, and 6b).

Source and Migration of Gases

Stable isotopes of carbon are commonly used to determine the source of CO_2 . Atmospheric CO_2 has a $\delta^{13}\text{C}\text{-CO}_2$ value of -8 per mil, which leads to air-saturated water with a $\delta^{13}\text{C}\text{-CO}_2$ value of ~ 0 (-2 to +2) per mil in subducted marine carbonate minerals (Craig, 1953). Microbial CO_2 derived from the oxidation of plant matter yields $\delta^{13}\text{C}\text{-CO}_2$ ranging between -26 to -22 per mil in rocks deposited before the Miocene (Quade et al., 1992). Similarly, the oxidation of petroleum or kerogen *in situ* yields $\delta^{13}\text{C}\text{-CO}_2$ that ranges from -26 to -16 per mil on average (Prinzhofer et al, 1995).

A combination of $\delta^{13}\text{C}\text{-CO}_2$ with $\text{CO}_2/^3\text{He}$ provides further insights to the source of the carbon dioxide and differentiates between isotope parameters indicative of gas source and those fractionated by water-rock interactions in the subsurface. A plot of $\delta^{13}\text{C}\text{-CO}_2$ vs. $\text{CO}_2/^3\text{He}$ shows that the majority of samples plot along a two component mixture between mantle-derived fluids sampled

from the Nyiragongo crater ($\text{CO}_2/^3\text{He} = 2\text{--}3 \times 10^{10}$ and $\delta^{13}\text{C}\text{-CO}_2 = -3.8$ per mil) and a trend of "water washing" (down to the left) (Figure 8).

During fluid migration, water-washing causes the physical alteration of the volcanic gases in the water-saturated crust by solubility partitioning. As the gases travel farther away from the source (in this case, the crater), the more soluble gases (i.e., CO_2) dissolve into the groundwater while the less soluble gases (i.e., He) remain in the gas phase, causing them to be enriched in the migrating phase. These results are consistent with previous observations in other field sites (Gilfillan et al., 2008; 2009). In general, the $\delta^{13}\text{C}$ values become isotopically lighter as the samples are collected farther away from the crater. Two samples showed an increase in the $\text{CO}_2/^3\text{He}$ ratio. The increased $\text{CO}_2/^3\text{He}$ ratios resulted either from the thermal alteration of carbonates or more likely the oxidation of organic matter (i.e., increasing CO_2 without additional ^3He). Together these data preclude microbial alteration as a source of carbon dioxide and suggest that mantle-derived fluids are the more likely source of carbon dioxide.

Discussion

Source Rock Composition

Volcanic rocks from the VVP are distinctive because of their unique silica undersaturated lavas that are found in no other terrestrial silicic volcanics (Chakrabarti, 2009). The lavas also are unusually high in alkalinity, with some samples reaching 14 combined weight % $\text{Na}_2\text{O} + \text{K}_2\text{O}$ (Figure 2). Although most terrestrial volcanic samples show a positive correlation between $\text{Na}_2\text{O} + \text{K}_2\text{O}$ vs. SiO_2 , the VVP samples have a negative correlation, with the alkalinity increasing while the silica content progressively decreases.

While the more recent lavas show little variation in alkalis, the older lavas of Nyiragongo show variable bulk rock chemistry, generally with lower total alkalis and slightly higher SiO_2 , similar to the more recent lava compositions. Following the 2002 eruption, the Mt. Nyiragongo lavas have continued to trend toward carbonatitic extremes for silica-undersaturated, alkali-rich rocks. While the source for this chemistry remains unclear, trace element and noble gas signatures may provide additional insight.

Chondrite-normalized rare earth element (REE) patterns are commonly used to calculate the degree of partial melting. The REE and high field strength element (HFSE) chemistry suggests that the composition of VVP lavas are due to metasomatism. The REE plot (Figure 3) shows a Gd anomaly, which most likely reflects either sub-continental lithospheric mantle or recycled Proterozoic crust. Because of the proximity of the VVP to the ancient suture zone between the Nubian Plate and the Tanzania Craton ($\sim 2\text{Ga}$), metasomatism of previously subducted crust may not be out of the realm of possibilities.

In addition to the REEs, other trace element ratios, including Th/U , Nb/U , and Zr/Hf , were calculated to distinguish the source and degree of metasomatism in the VVP. When metasomatism occurs, the Th/U and Nb/U decrease (an increase in $[\text{U}]$), while Zr/Hf increase ($[\text{Zr}]$ increases). Trace element fractionation related to metasomatism can be shown by plotting Th/U vs. Zr/Hf because of

their negative correlation (Figure 4). Based on the combination of the major elements, LREEs, the Gd anomaly, and high field strength elements such as Zr/Hf and Th/U we conclude that the composition of VVP lavas are due, at least in part, to metasomatism.

Variability in Metasomatic Influence over Time

The lava chemistry also shows the varying degree of metasomatism, with an increasing degree (down to the right) shown in the pre-1977 lavas, and a decreasing degree (up to the left) following the 2002 eruption of Mt. Nyiragongo (Figure 4). The Zr/Hf, Nb/U, and Th/U ratios were all plotted versus time along with $^3\text{He}/^4\text{He}$ (Figure 5). The $^3\text{He}/^4\text{He}$ values from the gases show this same pattern as the trace element ratios (Figures 6a and 6b). Even in 2002 when the degree of metasomatism, as inferred from the trace element ratios, was at its peak, the $^3\text{He}/^4\text{He}$ showed values similar to upper MORBs ($\sim 8R_a$) and then started to drop back down and return to a value consistent with sub-continental lithospheric mantle ($\sim 6.5R_a$). This seems to suggest that a deep seated plume underneath the VVP is not likely, but instead the lavas represent a mixture from complex and dynamic melting in the mantle related to two sources: a mid-ocean ridge basalt and sub-continental lithosphere.

Gas Migration

The majority of the samples plot along a two component mixture between mantle-derived fluids sampled from the Nyiragongo crater ($\text{CO}_2/^3\text{He} = 2\text{--}3 \times 10^{10}$ and $\delta^{13}\text{C-CO}_2 = -3.8$ per mil) (Figure 8). While normal mantle ratio for $\text{CO}_2/^3\text{He}$ is about 2×10^9 , many alkaline rich samples, like the ones from the VVP, typically have higher values. As there is not a substantial source of ^3He within the crust, and as ^3He is inert and highly insoluble, the variation in this ratio must be due to fluctuations in the CO_2 component within the reservoirs. Although many sources and sinks of CO_2 exist, the variation in the $\text{CO}_2/^3\text{He}$ ratios in this case is caused by CO_2 loss from the reservoir.

The $\text{CO}_2/{}^3\text{He}$ ratio is at its highest in the crater samples and then decreases in the samples with increasing distance from the crater, as the result of a process called “water-washing” (Figure 8). Water-washing is defined by the physical alteration of the volcanic gases in the water-saturated crust by solubility partitioning and occurs during fluid migration. As the gases travel farther away from the source (in this case, the crater), the more soluble gases (i.e. CO_2) dissolve into the groundwater while the less soluble gases (He) remain, causing them to be enriched in the migrating phase.

Without comparing the CO_2 concentrations to the helium, one would only have the $\delta^{13}\text{C}\text{-CO}_2$ values trending lighter as the samples were collected farther away from the crater, which could have been misconstrued as being due to microbial activity (Figure 8). The small trend (up to the left) on the other hand does show the addition of microbially-derived or organic CO_2 because of the $\text{CO}_2/{}^3\text{He}$ increase while also having lighter $\delta^{13}\text{C}\text{-CO}_2$ values, and is likely caused by oxidation of organic matter proximal to those samples because of the lighter $\delta^{13}\text{C}\text{-CO}_2$. These results are consistent with previous observations (Gilfillan et al, 2009).

Conclusions

The fumaroles throughout the Virunga Volcanic Province provide valuable information about the sources and migrational history within a geologically distinctive segment of the East African Rift System. The silica undersaturated and super-alkaline volcanics have a negative correlation between $\text{Na}_2\text{O} + \text{K}_2\text{O}$ and SiO_2 , and plot toward rare carbonatite lavas. Extreme LREE enrichment suggest the VVP rocks have undergone extreme mantle metasomatism, and the Gd anomaly reflects sub-continental lithospheric mantle or recycled Proterozoic crust, which is likely due to the VVP's proximity to a previous suture zone. The trace element ratios show a varying degree of metasomatism, but at the highest degree of metasomatism the $^3\text{He}/^4\text{He}$ ratio only reached upper MORB levels, suggesting a complex mantle melt is more likely than a deep seated plume. The $\delta^{13}\text{C}\text{-CO}_2$ values became lighter with increasing distance from the Nyiragongo crater as a result of the process of water washing as shown by the decrease in the $\text{CO}_2/^3\text{He}$ ratio.

In the future, more complete analyses of both the rock and gas samples could be done, looking at more potential ratios that could potentially show more evidence for metasomatism. The results from the Virunga Volcanic Province could also be compared to other large CO_2 reservoirs around the world with similar geologic settings, including McElmo Dome in the Four Corners (USA) and Jackson Dome in Mississippi (USA).

References

- Aguilera, F., Tassi, F., Darrah, T., Moune, S., Vaselli, O., 2012. Geochemical model of a magmatic-hydrothermal system at the Lastarria volcano, northern Chile. *Bulletin of Volcanology*, v. 74, p. 119–134.
- Ballentine, C.J., Burnard, P.G., 2002. Production, release, and transport of noble gases in the continental crust. *Reviews in Mineralogy and Geochemistry*, v. 47, p. 481–538.
- Ballentine, C.J., O’Nions, R.K., Oxburgh, E.R., Horvath, F., Deak, J., 1991. Rare-gas constraints on hydrocarbon accumulation, crustal degassing and groundwater-flow in the Pannonian Basin. *Earth and Planetary Science Letters*, v. 105, p. 229–246.
- Bondor, P.L., 1992. Applications of carbon dioxide in enhanced oil recovery. *Energy Convers*, v. 33, p. 579–586.
- Capaccioni, B., Aguilera, F., Tassi, F., Darrah, T.H., Poreda, R.J., Vaselli, O., 2011. Geochemical and isotopic evidences of magmatic inputs in the hydrothermal reservoir feeding the fumarolic discharges of Tacora volcano (northern Chile). *Journal of Volcanology and Geothermal Research*, v. 208, p. 77–85.
- Chakrabarti, R., Basu A., Santo, A., Tedesco, D., Vaselli, O., 2009. Isotopic and geochemical evidence for a heterogenous mantle plume origin of the Virunga volcanics, western rift, and East African Rift System. *Chemical Geology*, v. 259, p. 273–289.
- Clarke, W.B., Beg, M.A., Craig, H., 1969. Excess ^3He in the sea: evidence for terrestrial primordial helium. *Earth and Planetary Science Letters*, v. 6, p. 213–220.
- Craig, H., 1953. The geochemistry of the stable carbon isotopes. *Geochimica et Cosmochimica Acta*, v. 3, p. 53–92.
- Craig, H., Weiss, R.F., 1971. Dissolved gas saturation anomalies and excess helium in the ocean. *Earth and Planetary Science Letters*, v. 10, p. 289–296.
- Darrah, T.H., Poreda, R.J., 2012. Evaluating the accretion of meteoric debris and interplanetary dust particles in the GPC-3 sediment core using noble gas and mineralogical tracers. *Geochimica et Cosmochimica Acta*, v. 84, p. 329–352.
- Darrah, T.H., Tedesco, D., Tassi, F., Vaselli, O., Cuoco, E., Poreda, R.J., 2013. Gas chemistry of the Dallol region of the Danakil Depression in the Afar region of the northern-most East African Rift. *Chemical Geology*, v. 339, p. 16–29.
- Fischer, T.P., Burnard, P., Marty, B., Hilton, D.R., Furi, E., Palhol, F., Sharp, Z.D., Mangasini, F., 2009. Upper-mantle volatile chemistry at Oldoinyo Lengai volcano and the origin of carbonatites. *Nature*, v. 459, p. 77–80.

- Furman, T., 2007. Geochemistry of East African Rift basalts: an overview. *Journal of African Earth Sciences*, v. 48, p. 147-160.
- Giggenbach, W.F., Goguel, R.L., 1989. Collection and analysis of geothermal and volcanic water and gas discharges. New Zealand Department of Scientific and Industrial Research (Report No: CD2401), p. 1–81.
- Gilfillan, S.M.V., Ballentine, C.J., Holland, G., Blagburn, D., Sherwood-Lollar, B., Stevens, S., Martin, S., Martin, C., 2008. The noble gas geochemistry of natural CO₂ gas reservoirs from the Colorado Plateau and Rocky Mountain provinces, USA. *Geochimica et Cosmochimica Acta*, v. 72, p. 1174-1198.
- Gilfillan, S.M.V., Sherwood-Lollar, B., Holland, G., Blagburn, D., Stevens, S., Schoell, M., Cassidy, M., Ding, Z., Zhou, Z., Lacrampe-Couloume, G., Ballentine, C.J., 2009. Solubility trapping in formation water as dominant CO₂ sink in natural gas fields. *Nature*, v. 458, p. 614-618.
- Hunt, A.G., Darrah, T.H., Poreda, R.J., 2012. Determining the source and genetic fingerprint of natural gases using noble gas geochemistry: a northern Appalachian Basin case study. *AAPG Bulletin*, v. 96, p. 1785-1811.
- Jenden, P.D., Hilton, D.R., Kaplan, I.R., Craig, H. (Eds.), 1993. Abiogenic Hydrocarbons and Mantle Helium in Oil and Gas Fields. USGS Professional Paper, v. 1570, p. 31–56.
- LeMaitre, R.W., 1984. A proposal by the IUGS Subcommittee on the Systematics of igneous rocks for a chemical classification of volcanic rocks based on the total alkali silica (TAS) diagram. *Australian Journal of Earth Sciences*, v. 31, issue 2.
- Lupton, J.E., Craig, H., 1975. *Earth and Planetary Science Letters*, v. 26, p. 133-139.
- Montegrossi, G., Tassi, F., Vaselli, O., Buccianti, A., Garofalo, K., 2001. Sulfur Species in Volcanic Gases. *Analytical Chemistry*, v. 73, p. 3709-3715.
- Poreda, R.J., Farley, K.A., 1992. Rare gases in Samoan xenoliths. *Earth and Planetary Science Letters*, v. 113, p. 129-144.
- Prinzhofer, A.A., Huc, A.Y., 1995. Genetic and post-genetic molecular and isotopic fractionations in natural gases. *Chemical Geology*, v. 126, p. 281-290.
- Quade, J., Cerling, T.E., Barry, J.C., Morgan, M.E., Pilbeam, D.R., Chivas, A.R., Lee-Thorpe, J.A., Van der Merwe, N.J., 1992. A 16-Ma record of paleodiet using carbon and oxygen isotopes in fossil teeth in Pakistan, *Chemical Geology: Isotope Geoscience section*, v. 94, p. 183-192.
- Sherwood-Lollar, B., Ballentine, C.J., 2009. Insights into deep carbon derived from noble gases. *Nature Geoscience*, v. 2, p.543-547.

- Taylor, S.R., McLennan, S.M., 1995. The geochemical evolution of the continental crust. *Reviews of Geophysics*, v. 33, p. 241-265.
- Tedesco, D., 1994. Chemical and isotopic gas emissions at Campi Flegrei—evidence for an aborted period of unrest. *Journal of Geophysical Research—Solid Earth*, v. 99, p. 15623–15631.
- Tedesco, D., Tassi, F., Vaselli, O., Poreda, R.J., Darrah, T.H., Cuoco, E., Yalire, M.M., 2010. Gas isotopic signatures (He, C, and Ar) in the Lake Kivu region (western branch of the East African Rift System): geodynamic and volcanological implications. *Journal of Geophysical Research: Solid Earth*, v. 115, issue B1.
- Tassi, F., Aguilera, F., Darrah, T.H., Vaselli, O., Capaccioni, B., Poreda, R.J., Delgado Huertas, A., 2010. Fluid geochemistry of hydrothermal systems in the Arica Parinacota, Tarapaca and Antofagasta regions (northern Chile). *Journal of Volcanology and Geothermal Research*, v. 192, p. 1–15.
- Tassi, F., Aguilera, F., Vaselli, O., Darrah, T., Medina, E., 2011. Gas discharges from four remote volcanoes in northern Chile (Putana, Olca, Irruputuncu and Alitar): a geochemical survey. *Annals of Geophysics*, v. 54, p. 121–136.
- U.S. Department of Energy, National Energy Technology Laboratory. (2014). Near-Term Projections of CO₂ Utilization for Enhanced Oil Recovery (DOE/NETL-2014/1648).
- U.S. Department of Energy, National Energy Technology Laboratory. (2014). Subsurface Sources of CO₂ in the Contiguous United States (DOE/NETL-2014/1637).
- Zhou, Z., Ballentine, C.J., Schoell, M., Stevens, S.H., 2012. Identifying and quantifying natural CO₂ sequestration processes over geological timescales: the Jackson Dome CO₂ Deposit, USA. *Geochimica et Cosmochimica Acta*, v. 86, p. 257-275.



Figure 1a and 1b. The VVP is located on the border of DRC and Rwanda, along the western branch of the East African Rift System.

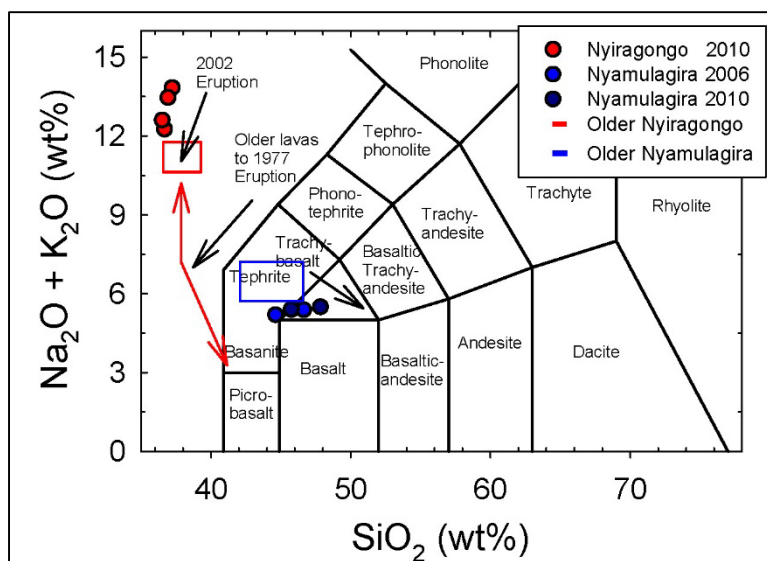


Figure 2. Total Alkali Silica Diagram of Nyiragongo and Nyamuragira during several eruptions and several samples, some of which were older with unknown eruption times (Chakrabarti et al., 2009).

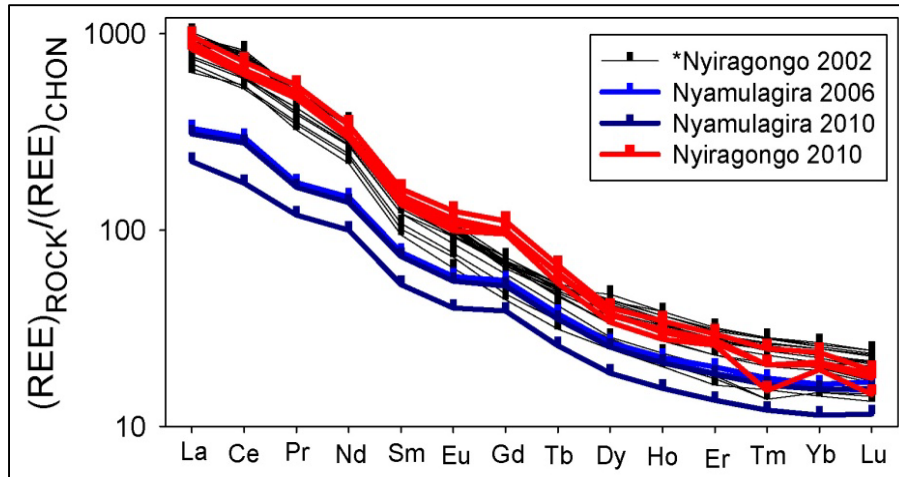


Figure 3. Chondrite (CHON) normalized rare earth element (REE) patterns of Nyiragongo and Nyamuragira.

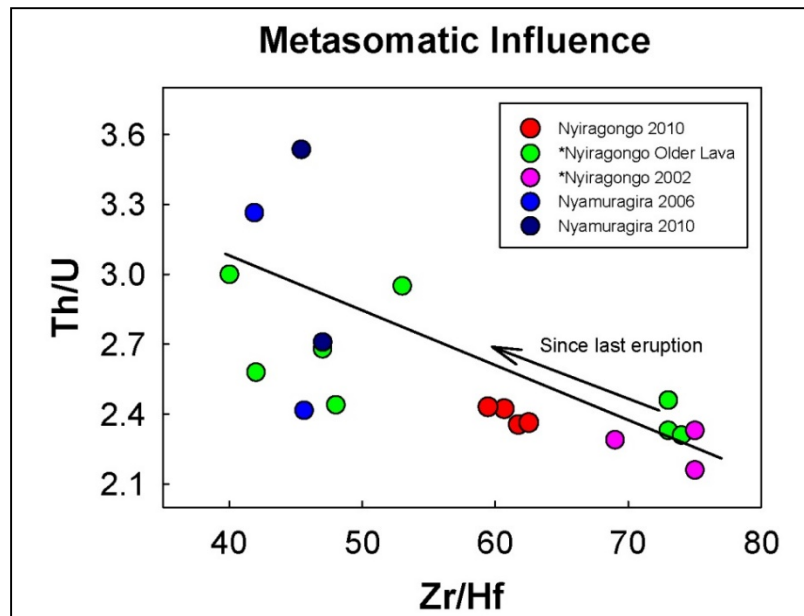


Figure 4. Th/U and Zr/Hf during several sampling expeditions.

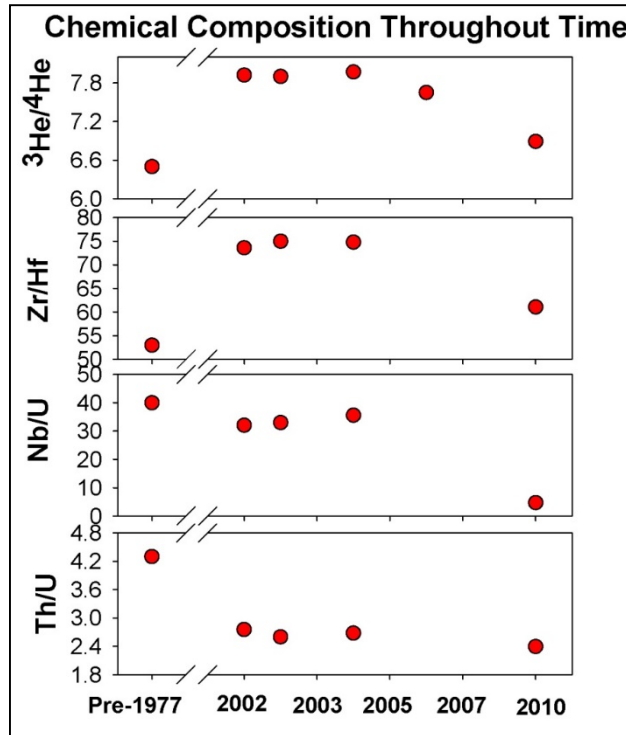


Figure 5. He and trace element ratios through time. The helium isotopic ratios show a corresponding trend to periods of peak metasomatism. At the peak, the $^3\text{He}/^4\text{He}$ ratio only reached upper MORB levels, suggesting a complex mantle melt is more likely than a deep seated plume.

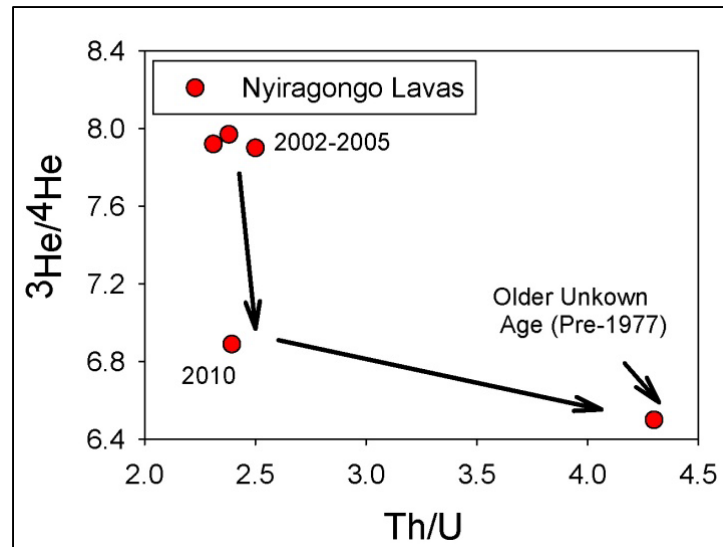
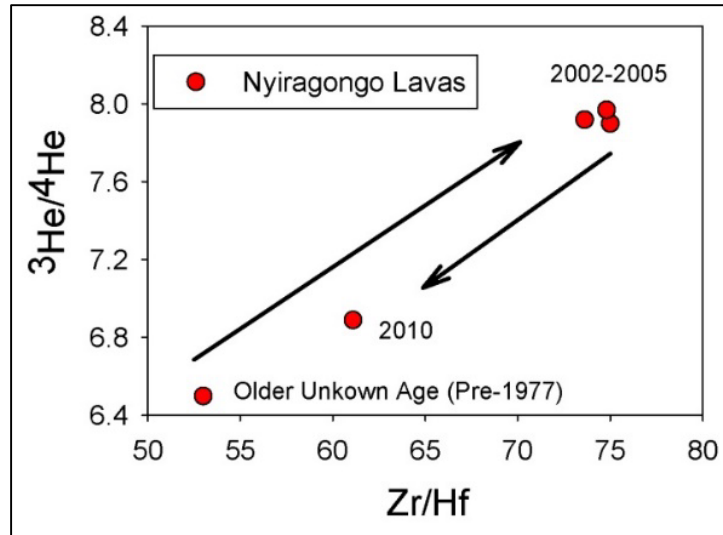


Figure 6a and 6b. $^3\text{He}/^4\text{He}$ vs. Zr/Hf and Th/U in the Nyiragongo lavas. The helium isotopic composition is consistent with trace element proxies for mantle metasomatism.

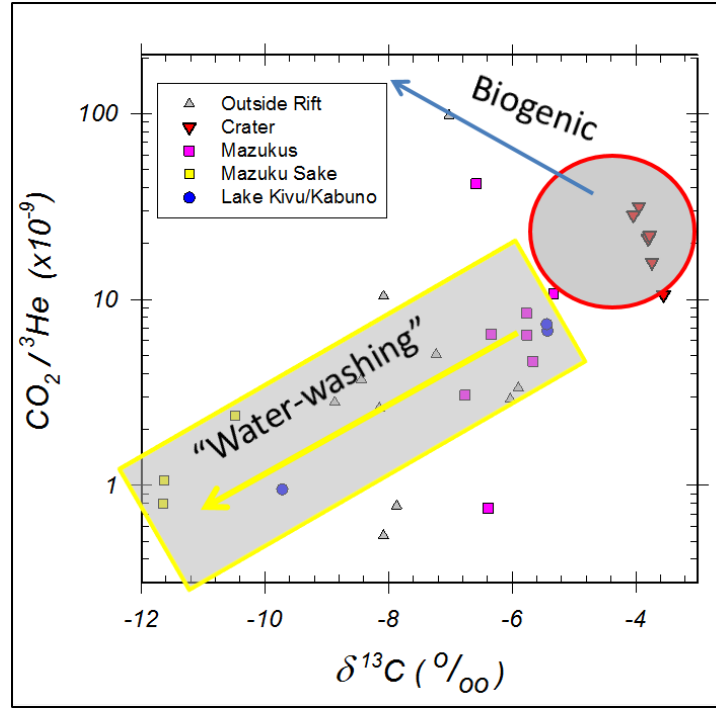


Figure 7. $\text{CO}_2/{}^3\text{He}$ vs. $\delta^{13}\text{C-CO}_2$. Volcano shows a $\text{CO}_2/{}^3\text{He}$ consistent with volcanic gases from silica undersaturated rock. Note that the bottom right red triangles are the most mantle-like end-member and that the trend in those samples is degassing of the magma body feeding the volcano. The trend to the bottom left is direct injection of CO_2 into the crust near the volcanic rift. The trend is shown by water-gas interactions as a result of differing solubility of each of the gases (${}^{12}\text{C-CO}_2$ vs ${}^{13}\text{C-CO}_2$ and CO_2 to ${}^3\text{He}$).